Real-Time Stabilization and Tracking of a Four-Rotor Mini Rotorcraft

Pedro Castillo, *Student Member, IEEE*, Alejandro Dzul, *Member, IEEE*, and Rogelio Lozano, *Member, IEEE*

***Abstract*—In this paper, we present a controller design and its implementation on a mini rotorcraft having four rotors. The dynamic model of the four-rotor rotorcraft is obtained via a Lagrange approach. The proposed controller is based on Lyapunov analysis using a nested saturation algorithm. The global stability analysis of the closed-loop system is presented. Real-time experiments show that the controller is able to perform autonomously the tasks of taking off, hovering, and landing.**

***Index Terms*—Aircraft control, aircraft dynamics, helicopter control, Lyapunov methods, real-time systems, recursive control algorithms.**

I. Introduction

THE automatic control of flying machines has attracted the attention of many researches in the past few years. Generally, the control strategies are based on simplified models which have both a minimum number of states and a minimum number of inputs. These reduced models should retain the main features that must be considered when designing control laws for real aerial vehicles. In this paper, we are interested in the design of a relatively simple control algorithm to perform hover and tracking of desired trajectories.

The rotorcraft is one of the most complex flying machines. Its complexity is due to the versatility and maneuverability to perform many types of tasks [1]. The classical helicopter is conventionally equipped with a main rotor and a tail rotor. However, other types of helicopters exist, including the twin rotor or tandem helicopter and the coaxial rotor helicopter. In this paper, we are particularly interested in controlling a mini rotorcraft having four rotors.

Four-rotor rotorcrafts, like the one shown in Fig. 1, have some advantages over conventional helicopters. Given that the front and rear motors rotate counterclockwise while the other two rotate clockwise, gyroscopic effects and aerodynamic torques tend to cancel in trimmed flight.

This four-rotor rotorcraft does not have a swashplate. In fact it does not need any blade pitch control. The collective input (or throttle input) is the sum of the thrusts of each motor. Pitch movement is obtained by increasing (reducing) the speed of the rear motor while reducing (increasing) the speed of the front motor. The roll movement is obtained similarly using the lateral motors. The yaw movement is obtained by increasing (decreasing) the speed of the front and rear motors while decreasing (increasing) the speed of the lateral motors. This should be done while keeping the total thrust constant.

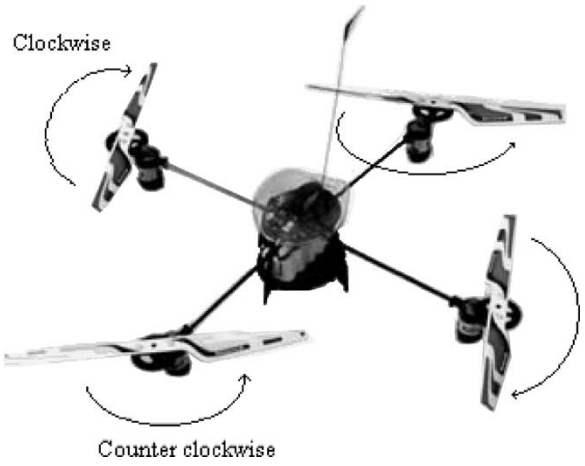

Fig. 1. The four-rotor rotorcraft.

In view of its configuration, the four-rotor rotorcraft in Fig. 1 has some similarities with planar vertical take off and landing (PVTOL) aircraft problem [2], [6], [7]. The PVTOL is a mathematical model of a flying object that evolves in a vertical plane. It has three degrees of freedom (x, y, and θ) corresponding to its position and orientation in the plane. The PVTOL is composed of two independent thrusters that produce a force and a moment on the flying machine, see Fig. 2. The PVTOL is an underactuated system since it has three degrees of freedom and only two inputs. The PVTOL is a very interesting nonlinear control problem. Furthermore, the four-rotor rotorcraft reduces to a PVTOL when the roll and yaw angles are set to zero. In a way, the four-rotor rotorcraft can be seen as two PVTOL connected such that their axes are orthogonal.

In this paper, we present the model of a four-rotor rotorcraft whose dynamical model is obtained via a Lagrange approach [5]. A control strategy is proposed having in mind that the four-rotor rotorcraft can be seen as the interconnection of two PVTOL aircraft. Indeed, we first design a control to stabilize the yaw angular displacement. We then control the pitch movement using a controller based on the dynamic model of a PVTOL [2]. Finally, the roll movement is controlled using again a strategy based on the PVTOL.

The control algorithm is based on the nested saturation control strategy proposed by [3] and discussed for general nonlinear systems, including the PVTOL, in [10]. We prove global

Manuscript received July 10, 2002; revised July 4, 2003. Manuscript received in final form October 10, 2003. Recommended by Associate Editor J. M. Buffington.

P. Castillo and R. Lozano are with the Heudiasyc UMR-CNRS 6599, Université de Technologie de Compiègne, Centre de Recherche de Royallieu, 60200 Compiègne, Cedex, France (e-mail: castillo@hds.utc.fr; rlozano@hds.utc.fr).

A. Dzul is with the División de Estudios de Posgrado e Investigación, Instituto Tecnológico de la Laguna, 27000 Torreón, Coahuila, Mexico (e-mail: dzul@hds.utc.fr).

Digital Object Identifier 10.1109/TCST.2004.825052

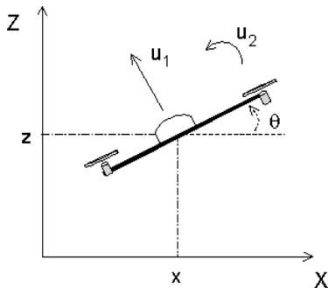

Fig. 2. The PVTOL aircraft.

stability of the proposed controller. Furthermore, the controller has been implemented on a PC and real-time experiments have shown that the proposed control strategy performs well in practice. Robustness with respect to parameter uncertainty and unmodeled dynamics has been observed in a real-time application performed by the aerial control team at the University of Technology, Compiègne, France.

The paper is organized as follows. The problem statement is presented in Section II. Section III describes the control law design. In Section IV, we present the experimental results and finally, some conclusions are given in Section V.

II. Problem Statement

In this section, we present the model of the four-rotor rotorcraft using a Lagrangian approach. The generalized coordinates for the rotorcraft are

$$q = (x, y, z, \psi, \theta, \phi) \in \Re^6$$

where (x, y, and z) denote the position of the center of mass of the four-rotor rotorcraft relative to the frame $\mathcal{I}$ and (ψ, θ, ϕ) are the three Euler angles (yaw, pitch, and roll angles) and represent the orientation of the rotorcraft [8], [9].

Therefore, the model partitions naturally into translational and rotational coordinates

$$\xi = (x, y, z) \in \Re^3, \quad \eta = (\psi, \theta, \phi) \in \Re^3.$$

The translational kinetic energy of the rotorcraft is

$$T_{\text{trans}} \triangleq \frac{m}{2}\dot{\xi}^T\dot{\xi} \tag{1}$$

where m denotes the mass of the rotorcraft. The rotational kinetic energy is

$$T_{\text{rot}} \triangleq \frac{1}{2}\dot{\eta}^T \mathbb{J}\dot{\eta}. \tag{2}$$

The matrix $\mathbb{J}$ acts as the inertia matrix for the full-rotational kinetic energy of the rotorcraft expressed directly in terms of the generalized coordinates η. The only potential energy which needs to be considered is the standard gravitational potential given by

$$U = mgz. \tag{3}$$

The Lagrangian is

$$\begin{aligned} L(q, \dot{q}) &= T_{\text{trans}} + T_{\text{rot}} - U \\ &= \frac{m}{2}\dot{\xi}^T\dot{\xi} + \frac{1}{2}\dot{\eta}^T\mathbb{J}\dot{\eta} - mgz. \end{aligned} \tag{4}$$

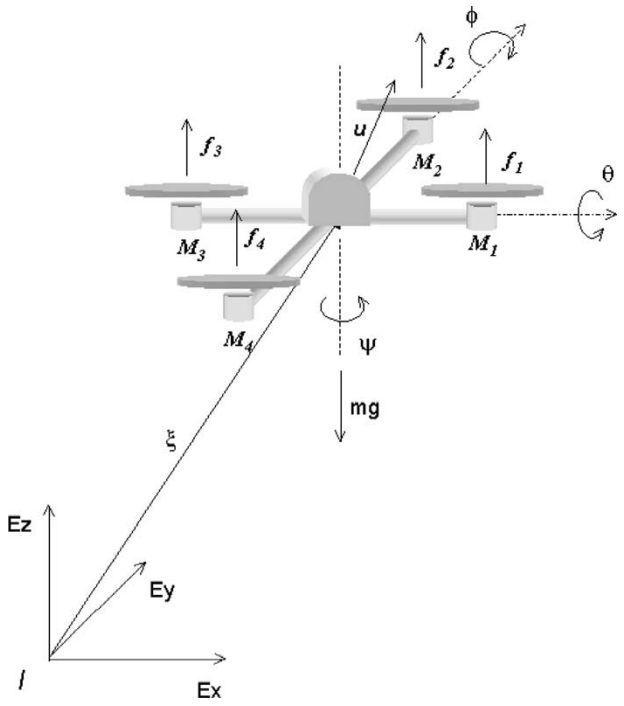

Fig. 3. Schema of the four-rotor rotorcraft.

The model for the full rotorcraft dynamics is obtained from the Euler–Lagrange equations with external generalized force

$$\frac{d}{dt}\frac{\partial \mathcal{L}}{\partial \dot{q}} - \frac{\partial \mathcal{L}}{\partial q} = F$$

where $F = (F_\xi, \tau)$ and τ is the generalized moments. F_ξ is the translational force applied to the rotorcraft due to the control inputs. We ignore the small body forces because they are generally of a much smaller magnitude than the principal control inputs u and τ then we write

$$\widehat{F} = \begin{pmatrix} 0 \\ 0 \\ u \end{pmatrix} \tag{5}$$

where (see Fig. 3)

$$u = f_1 + f_2 + f_3 + f_4$$

and

$$f_i = k_i w_i^2, \quad i = 1, \ldots 4$$

where $k_i > 0$ is a constant and w_i is the angular speed of motor "i" (M_i, $i = 1, \ldots 4$), then

$$F_\xi = R\widehat{F} \tag{6}$$

where R is the transformation matrix representing the orientation of the rotorcraft. We use c_θ for $\cos\theta$ and s_θ for $\sin\theta$.

$$R = \begin{pmatrix} c_\theta c_\psi & s_\psi s_\theta & -s_\theta \\ c_\psi s_\theta s_\phi - s_\psi c_\phi & s_\psi s_\theta s_\phi + c_\psi c_\phi & c_\theta s_\phi \\ c_\psi s_\theta c_\phi + s_\psi s_\phi & s_\psi s_\theta c_\phi - c_\psi s_\phi & c_\theta c_\phi \end{pmatrix}$$

The generalized moments on the η variables are

$$\tau \triangleq \begin{pmatrix} \tau_\psi \\ \tau_\theta \\ \tau_\phi \end{pmatrix} \tag{7}$$

where

$$\tau_\psi = \sum_{i=1}^{4} \tau_{M_i}$$
$$\tau_\theta = (f_2 - f_4)\ell$$
$$\tau_\phi = (f_3 - f_1)\ell$$

where ℓ is the distance from the motors to the center of gravity and τ_{M_i} is the couple produced by motor M_i.

Since the Lagrangian contains no cross terms in the kinetic energy combining $\dot{\xi}$ and $\dot{\eta}$ (4), the Euler–Lagrange equation can be partitioned into the dynamics for the ξ coordinates and the η dynamics. One obtains

$$m\ddot{\xi} + \begin{pmatrix} 0 \\ 0 \\ mg \end{pmatrix} = F_\xi \tag{8}$$

$$\mathbb{J}\ddot{\eta} + \dot{\mathbb{J}}\dot{\eta} - \frac{1}{2}\frac{\partial}{\partial \eta}(\dot{\eta}^T \mathbb{J}\dot{\eta}) = \tau. \tag{9}$$

Defining the Coriolis–Centripetal vector

$$\bar{V}(\eta, \dot{\eta}) = \dot{\mathbb{J}}\dot{\eta} - \frac{1}{2}\frac{\partial}{\partial \eta}(\dot{\eta}^T \mathbb{J}\dot{\eta}) \tag{10}$$

we may write

$$\mathbb{J}\ddot{\eta} + \bar{V}(\eta, \dot{\eta}) = \tau \tag{11}$$

but we can rewrite $\bar{V}(\eta, \dot{\eta})$ as

$$\begin{aligned} \bar{V}(\eta, \dot{\eta}) &= \left(\dot{\mathbb{J}} - \frac{1}{2}\frac{\partial}{\partial \eta}(\dot{\eta}^T \mathbb{J})\right)\dot{\eta} \\ &= C(\eta, \dot{\eta})\dot{\eta} \end{aligned} \tag{12}$$

where $C(\eta, \dot{\eta})$ is referred to as the Coriolis terms and contains the gyroscopic and centrifugal terms associated with the η dependence of $\mathbb{J}$.

Finally, we obtain

$$m\ddot{\xi} = u \begin{pmatrix} -\sin\theta \\ \cos\theta \sin\phi \\ \cos\theta \cos\phi \end{pmatrix} + \begin{pmatrix} 0 \\ 0 \\ -mg \end{pmatrix} \tag{13}$$

$$\mathbb{J}\ddot{\eta} = -C(\eta, \dot{\eta})\dot{\eta} + \tau. \tag{14}$$

III. Control Law Design

In this section, we will develop a control strategy for stabilizing the four-rotor rotorcraft at hover. We will prove global stability of the closed-loop system. Furthermore, the proposed controller design is such that the resulting controller is relatively simple and each one of the control inputs can operate in either manual or automatic mode independently. For flight safety reasons this feature is particularly important when implementing the control strategy as will be explained in Section IV. The collective input "u" in (13) is essentially used to make the altitude reach a desired value. The control input τ_ψ is used to set the yaw displacement to zero. τ_θ is used to control the pitch and the horizontal movement in the x axis. Similarly, τ_ϕ is used to control the roll and horizontal displacement in the y axis.

In order to simplify let us propose a change of the input variables

$$\tau = C(\eta, \dot{\eta})\dot{\eta} + \mathbb{J}\tilde{\tau} \tag{15}$$

where

$$\tilde{\tau} = \begin{pmatrix} \tilde{\tau}_\psi \\ \tilde{\tau}_\theta \\ \tilde{\tau}_\phi \end{pmatrix} \tag{16}$$

are the new inputs. Then

$$\ddot{\eta} = \tilde{\tau}. \tag{17}$$

Rewriting (13), (14)

$$m\ddot{x} = -u\sin\theta \tag{18}$$
$$m\ddot{y} = u\cos\theta\sin\phi \tag{19}$$
$$m\ddot{z} = u\cos\theta\cos\phi - mg \tag{20}$$
$$\ddot{\psi} = \tilde{\tau}_\psi \tag{21}$$
$$\ddot{\theta} = \tilde{\tau}_\theta \tag{22}$$
$$\ddot{\phi} = \tilde{\tau}_\phi \tag{23}$$

where x and y are the coordinates in the horizontal plane, and z is the vertical position (see Fig. 3). ψ is the yaw angle around the z axis, θ is the pitch angle around the (new) y axis, and ϕ is the roll angle around the (new) x axis. The control inputs u, $\tilde{\tau}_\psi$, $\tilde{\tau}_\theta$ and $\tilde{\tau}_\phi$ are the total thrust or collective input (directed out the bottom of the aircraft) and the new angular moments (yawing moment, pitching moment and rolling moment).

A. Altitude and Yaw Control

The control of the vertical position can be obtained by using the following control input:

$$u = (r_1 + mg)\frac{1}{c_\theta c_\phi} \tag{24}$$

where

$$r_1 = -a_{z_1}\dot{z} - a_{z_2}(z - z_d) \tag{25}$$

where a_{z_1} and a_{z_2} are positive constants and z_d is the desired altitude. The yaw angular position can be controlled by applying

$$\tilde{\tau}_\psi = -a_{\psi_1}\dot{\psi} - a_{\psi_2}(\psi - \psi_d). \tag{26}$$

Indeed, introducing (24)–(26) into (18)–(21) and provided that $c_\theta c_\phi \neq 0$, we obtain

$$m\ddot{x} = -(r_1 + mg)\frac{\tan\theta}{\cos\phi} \tag{27}$$
$$m\ddot{y} = (r_1 + mg)\tan\phi \tag{28}$$
$$\ddot{z} = \frac{1}{m}\left(-a_{z_1}\dot{z} - a_{z_2}(z - z_d)\right) \tag{29}$$
$$\ddot{\psi} = -a_{\psi_1}\dot{\psi} - a_{\psi_2}(\psi - \psi_d). \tag{30}$$

The control parameters a_{ψ_1}, a_{ψ_2}, a_{z_1}, and a_{z_2} should be carefully chosen to ensure a stable well-damped response in the vertical and yaw axes.

From (29) and (30) it follows that $\psi \to \psi_d$ and $z \to z_d$.

B. Roll Control (ϕ, y)

Note that from (25) and (29) $r_1 \rightarrow 0$. For a time T large enough, r_1 and ψ are arbitrarily small, therefore, (27) and (28) reduce to

$$\ddot{x} = -g\frac{\tan\theta}{\cos\phi} \tag{31}$$

$$\ddot{y} = g\tan\phi. \tag{32}$$

We will first consider the subsystem given by (23) and (32). We will implement a nonlinear control based on nested saturations. This type of control allows in the limit a guarantee of arbitrary bounds for ϕ, $\dot{\phi}$, y, and $\dot{y}$. To further simplify the analysis we will impose a very small upper bound on $|\phi|$ in such a way that the difference $\tan(\phi) - \phi$ is arbitrarily small. Therefore, the subsystem (23)–(32) reduces to

$$\ddot{y} = g\phi \tag{33}$$

$$\ddot{\phi} = \tilde{\tau}_\phi \tag{34}$$

which represents four integrators in cascade. We can now use the technique developed in [3] based on nested saturations control to stabilize the four integrators in cascade. The controller is given as follows:

$$\tilde{\tau}_\phi = -\sigma_{\phi_1}\left(\dot{\phi} + \sigma_{\phi_2}\left(\phi + \dot{\phi} + \sigma_{\phi_3}\left(2\phi + \dot{\phi} + \frac{\dot{y}}{g} + \sigma_{\phi_4}\left(\dot{\phi} + 3\phi + 3\frac{\dot{y}}{g} + \frac{y}{g}\right)\right)\right)\right). \tag{35}$$

Using [3] we can prove that ϕ, $\dot{\phi}$, y and $\dot{y}$ converge to zero when applied to system (33) and (34). System (33) and (34) has been obtained by neglecting terms that converge to zero. In general, it is not true that stability is preserved in presence of terms converging to zero. Nevertheless, in our case, we can apply the robust stability result in [10] to guarantee that stability is preserved in spite of terms that converge to zero.

C. Pitch Control (θ, x)

From (33) and (35), we obtain $\phi \rightarrow 0$, then from (31) gives

$$\ddot{x} = -g\tan\theta. \tag{36}$$

Finally, we take the subsystem

$$\ddot{x} = -g\tan\theta \tag{37}$$

$$\ddot{\theta} = \tilde{\tau}_\theta. \tag{38}$$

As before, we assume that the control strategy will insure a very small bound on $|\theta|$ in such a way that $\tan(\theta) \approx \theta$. Therefore, (37) reduces to

$$\ddot{x} = -g\theta. \tag{39}$$

Using a procedure similar to the one proposed for the roll control we obtain

$$\tilde{\tau}_\theta = -\sigma_{\theta_1}\left(\dot{\theta} + \sigma_{\theta_2}\left(\theta + \dot{\theta} + \sigma_{\theta_3}\left(2\theta + \dot{\theta} - \frac{\dot{x}}{g} + \sigma_{\theta_4}\left(\dot{\theta} + 3\theta - 3\frac{\dot{x}}{g} - \frac{x}{g}\right)\right)\right)\right). \tag{40}$$

TABLE I
ROTORCRAFT PHYSICAL CHARACTERISTICS

Weight (not including batteries)	320 g
Batteries weight	200 g
Maximum length	74 cm
Blades diameter	29 cm
Height	11 cm
Distance between the motor and the C.G.	20.5 cm
Motor reduction rate	1:6

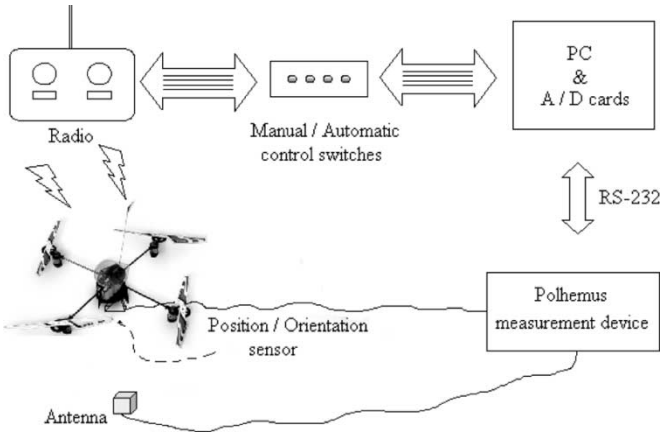

Fig. 4. Real-time architecture of the platform.

IV. EXPERIMENTAL RESULTS

In this section, we present the real-time experimental results obtained when applying the controller proposed in the previous section to a four-rotor mini rotorcraft. We will first describe the architecture of the platform and then explain how the controller parameters were tuned.

A. Platform Description

The flying machine we have used is a mini rotorcraft having four rotors manufactured by Draganfly Innovations, Inc. (http://www.rctoys.com). The physical characteristics of this rotorcraft are given in Table I.

The four control signals are transmitted by a Futaba Skysport 4 radio. The control signals are referred as throttle control input u, pitch control input $\tilde{\tau}_\theta$, roll control input $\tilde{\tau}_\phi$, and yaw control input $\tilde{\tau}_\psi$. These control signals are constrained in the radio to satisfy

$$\begin{aligned} 0.66\,[\mathrm{V}] < u < 4.70\,[\mathrm{V}] \\ 1.23\,[\mathrm{V}] < \tilde{\tau}_\theta < 4.16\,[\mathrm{V}] \\ 0.73\,[\mathrm{V}] < \tilde{\tau}_\phi < 4.50\,[\mathrm{V}] \\ 0.40\,[\mathrm{V}] < \tilde{\tau}_\psi < 4.16\,[\mathrm{V}]. \end{aligned} \tag{41}$$

The radio and the PC (INTEL Pentium 3) are connected using data acquisition cards (ADVANTECH PCL-818HG and PCL-726). The connection in the radio is directly made to the joystick potentiometers for the collective, yaw, pitch, and roll controls.

In order to simplify the tuning of the controller and for flight security reasons, we have introduced several switches in the PC-radio interface so that each control input can operate either in manual mode or in automatic control mode (see Fig. 4).

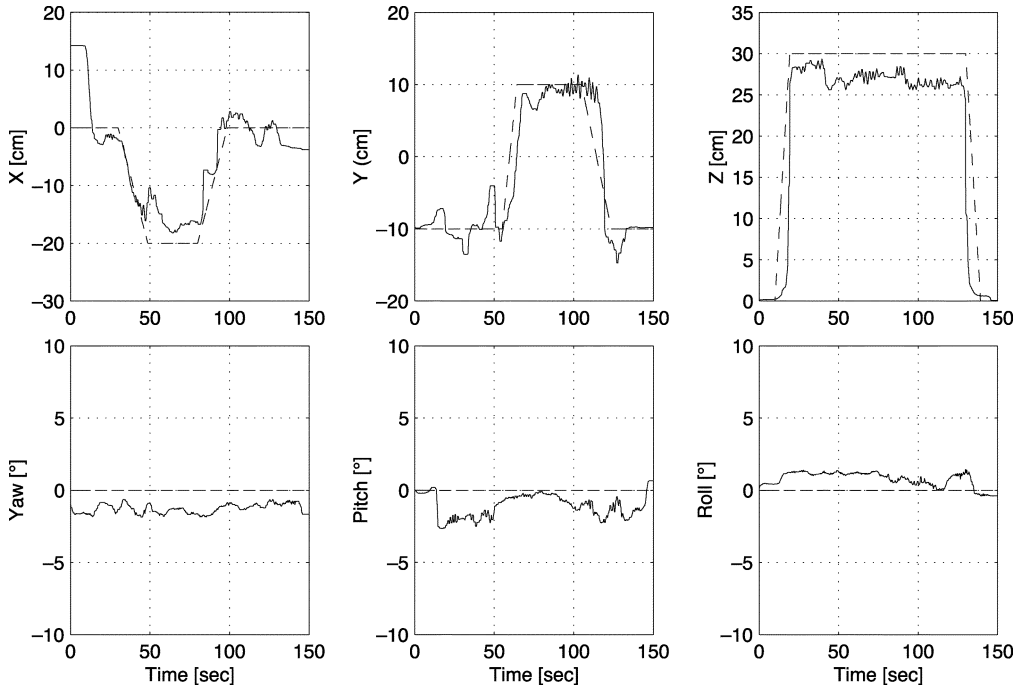

Fig. 5. Position (x, y, z) and orientation (ψ, θ, ϕ) of the four-rotor rotorcraft. The dotted lines represent the desired trajectories.

Therefore, we select the control inputs that are handled manually by the pilot while the other control inputs are provided by the computer.

In the first stage, only the yaw control input is controlled by the computer. After obtaining good performance in the yaw displacement we start dealing with the automatic control of the roll. In the third stage, only the throttle is handled by the pilot while in the last stage all the modes are controlled by the computer.

The rotorcraft revolves freely in three dimensional (3-D) space without any flying stand. To measure the position (x, y, z) and orientation (ψ, θ, ϕ) of the rotorcraft we use the 3-D tracker system (POLHEMUS) [4]. The Polhemus is connected via RS232 to the PC (see Fig. 4). This type of sensor is very sensitive to electromagnetic noise and we had to install it as far as possible from the electric motors and their drivers.

The Draganfly III has three onboard gyros that help stabilize the mini rotorcraft. It would be impossible for a pilot to stabilize this flying machine without gyro stabilization. It would be a very difficult task to deactivate the gyros and we think that since they work so well, it would not be reasonable to disconnect them. Thus, these three angular velocity feedbacks provided by the onboard gyros are considered as a in-built inner control loop. Notice that this gyro stabilization is not enough for performing hover autonomously.

The use of the Polhemus sensor allows the achievement of practical experiments on the laboratory. An actual unmanned autonomous vehicle (UAV) would require onboard inertial measurements to be able to fly outdoors.

B. Controller Parameters Tuning

The computation of the control input requires the knowledge of the various angular and linear velocities. The sensor that is at our disposal only measures position and orientation. We have thus computed estimates of the angular and linear velocities by using the following approximation:

$$\dot{q}_t = \frac{q_t - q_{t-T}}{T} \tag{42}$$

where q is a given variable and T is the sampling period. In our experiment $T = (1/14)s$ due to limitations imposed by the measuring device. In order to obtain a good estimate of the angular and linear velocities and avoid abrupt changes in these signals we have introduced numerical filters. We have used first-order numerical filters. The gain and the pole of each filter were selected to obtain improve the signal-to-noise ratio.

The controller parameters are selected using the following procedure. The yaw controller parameters are first tuned while the other modes are handled by the pilot. The yaw controller is basically a PD controller. The parameters are selected to obtain

TABLE II
GAIN VALUES USED IN THE CONTROL LAW

Phase	*Control parameter*	*Value*
1.- Altitude	a_{z_1}	0.001
	a_{z_2}	0.002
2.- Yaw control	a_{ψ_1}	2.374
	a_{ψ_2}	0.08
3.- Roll control	M_{ϕ_1}	2
	M_{ϕ_2}	1
	M_{ϕ_3}	0.2
	M_{ϕ_4}	0.1
4.- Pitch control	M_{θ_1}	2
	M_{θ_2}	1
	M_{θ_3}	0.2
	M_{θ_4}	0.1
$1-4$	T	$\frac{1}{14}s$

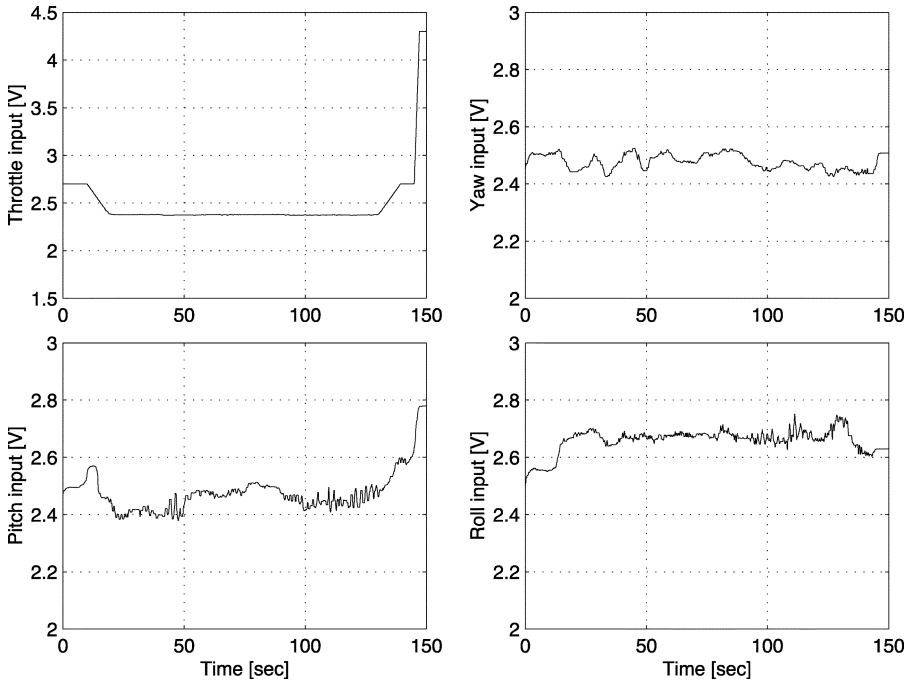

Fig. 6. Controls inputs (throttle input, yaw, pitch, and roll).

a short settling time without introducing small oscillations in the yaw displacement.

The yaw control input should also satisfy the constraints (41). The parameters of the roll control input are carried out while the throttle and pitch controls are in manual mode. The parameters of the roll control are adjusted in the following sequence. We first select the gain concerning roll angular velocity $\dot{\phi}$. Due to the on-board gyros, this gain is relatively small. We next select the controller gain concerning the roll displacement ϕ. We wish the roll error to converge to zero fast but without undesirable oscillations.

The controller gain concerning $\dot{y}$ and the amplitude of the saturation function are selected in such a way that the mini aircraft reduces its speed in the y axis fast enough. To complete the tuning of the roll control parameters we choose the gains concerning the y displacement to obtain a satisfactory performance. The parameters of the pitch control are selected similarly. Finally we tune the parameters of the throttle control to obtain a desired altitude. One of the controller parameters is used to compensate the gravity force which is estimated off-line using experimental data.

Notice that since this mini rotorcraft has soft blades, the tuning of the parameters can be done while holding the rotorcraft in the hand and wearing eyeprotection glasses. This certainly cannot be done with larger flying machines and, therefore, more simulation developments have to be performed before actually applying the controller to the real system. In our case, simulations were not required.

C. Experiment

The gain values used for the control law are shown in Table II.

The control objective is to make the mini rotorcraft hover at an altitude of 30 [cm], i.e., we wish to reach the position $(x, y, z) = (0, 0, 30\ \mathrm{cm})$, while $(\psi, \theta, \phi) = (0, 0, 0)$. We also make the rotorcraft follow a simple horizontal trajectory.

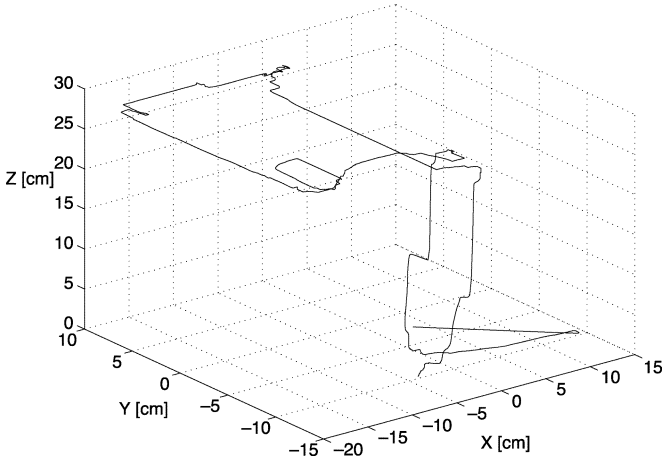

Fig. 7. 3-D motion of the rotorcraft.

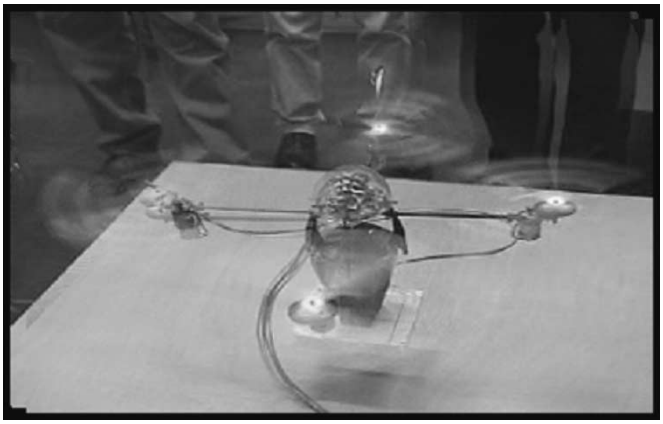

Fig. 8. The four-rotor rotorcraft hovering autonomously.

Figs. 5–7 show the performance of the controller when applied to the rotorcraft. Fig. 8 shows the four-rotor rotorcraft hovering autonomously. Videos of the

experiments can be seen in the following address: http://www.hds.utc.fr/~castillo/4r_fr.html

V. Conclusion

We have proposed a stabilization control algorithm for a mini rotorcraft having four rotors. The dynamic model of the rotorcraft was obtained via a Lagrange approach and the proposed control algorithm is based on nested saturations.

The proposed strategy has been successfully applied to the rotorcraft and the experimental results have shown that the controller performs satisfactorily.

To the best of our knowledge, this is the first successful real-time control applied to a four-rotor rotorcraft.

Acknowledgment

The authors wish to thank the reviewers for their valuable comments.

References

[1] W. Barnes and W. McCormick, *Aerodynamics Aeronautics and Flight Mechanics*. New York: Wiley, 1995.
[2] J. Hauser, S. Sastry, and G. Meyer, "Nonlinear control design for slightly nonminimum phase systems: application to V/STOL aircraft," *Automatica*, vol. 28, no. 4, pp. 665–679, 1992.
[3] A. R. Teel, "Global stabilization and restricted tracking for multiple integrators with bounded controls," *Syst. Control Lett.*, 1992.
[4] *Fastrack 3Space Polhemus User's Manual*, Colchester, VT, 2002.
[5] R. Lozano, B. Brogliato, O. Egeland, and B. Maschke, *Passivity-Based Control System Analysis and Design*, ser. Communications and Control Engineering Series. New York: Springer-Verlag, 2000, vol. ISBN: 1–85233–285–9.
[6] I. Fantoni and R. Lozano, *Control of Nonlinear Mechanical Underactuated Systems*, ser. Communications and Control Engineering Series. New York: Springer-Verlag, 2001.
[7] L. Marconi, A. Isidori, and A. Serrani, "Autonomous vertical landig on an oscillating platform: an internal-model based approach," *Automatica*, vol. 38, pp. 21–32, 2002.
[8] T. S. Alderete, *Simulator Aero Model Implementation*. Moffett Field, CA: NASA Ames Res. Ctr..
[9] B. Etkin, *Dynamics of Flight*. New York: Wiley, 1959.
[10] A. R. Teel, "A nonlinear small gain theorem for the analysis of control systems with saturation," *IEEE Trans Automat. Contr.*, vol. 41, pp. 1256–1270, Sept. 1996.

Pedro Castillo (S'04) was born in Morelos, Mexico, on January 8, 1975. He received the B.S. degree in electromechanic engineering from the Instituto Tecnologico de Zacatepec, Morelos, Mexico, in 1997, the M.Sc. degree in electrical engineering from the Centro de Investigación y de Estudios Avanzados (CINVESTAV), Mexico, in 2000, and the Ph.D. degree in automatic control from the University of Technology of Compiègne, France, in 2004.

His research topics include real-time control applications, nonlinear dynamics and control, aerospace vehicles, vision, and underactuated mechanical systems.

Alejandro Dzul (S'99–M'03) was born in Gomez Palacio, Mexico, on April 30, 1971. He received the B.S. degreee in electronic engineering and the M.S. degree in electrical engineering, both from Instituto Tecnológico de La Laguna, Mexico, in 1993 and 1997, respectively, and the Ph.D. degree in automatic control from Université de Technologie de Compiègne, France, in 2002.

He has been a Research Professor with the Electrical and Electronic Engineering Department at Instituto Tecnologico de La Laguna since 2003. His current research interests are in the areas of nonlinear dynamics and control and real-time control with applications to aerospace vehicles.

Rogelio Lozano (M'94) was born in Monterrey Mexico, on July 12, 1954. He received the B.S. degree in electronic engineering from the National Polytechnic Institute of Mexico, in 1975, the M.S. degree in electrical engineering from Centro de Investigación y de Estudios Avanzados (CIEA), Mexico, in 1977, and the Ph.D. degree in automatic control from Laboratoire d'Automatique de Grenoble, France, in 1981.

He joined the Department of Electrical Engineering at the CIEA, Mexico, in 1981, where he worked until 1989. He was a Visitor at the University of Newcastle, Australia, from 1983 to 1984, at NASA Langley Research Center, VA, from 1987 to 1988, and Laboratoire d'Automatique de Grenoble, France, from 1989 to 1990. Since 1990 he has been a CNRS Research Director at the University of Technology, Compiègne, France. He has been Head of the Laboratory Heudiasyc, UMR 6599 CNRS, since January 1995. He was Associate Editor of *Automatica* from 1987 to 2000 and of the *International Journal of Adaptive Control and Signal Processing* since 1993. His research interest are in adaptive control, passivity, nonlinear systems, underactuated mechanical systems, and autonomous helicopters.